

Tailored Excitation for Frequency Response Measurement Applied to the X-43A Flight Vehicle

*Ethan Baumann
NASA Dryden Flight Research Center
Edwards, California*

NASA STI Program ... in Profile

Since its founding, NASA has been dedicated to the advancement of aeronautics and space science. The NASA scientific and technical information (STI) program plays a key part in helping NASA maintain this important role.

The NASA STI program is operated under the auspices of the Agency Chief Information Officer. It collects, organizes, provides for archiving, and disseminates NASA's STI. The NASA STI program provides access to the NASA Aeronautics and Space Database and its public interface, the NASA Technical Report Server, thus providing one of the largest collections of aeronautical and space science STI in the world. Results are published in both non-NASA channels and by NASA in the NASA STI Report Series, which includes the following report types:

- **TECHNICAL PUBLICATION.** Reports of completed research or a major significant phase of research that present the results of NASA programs and include extensive data or theoretical analysis. Includes compilations of significant scientific and technical data and information deemed to be of continuing reference value. NASA counterpart of peer-reviewed formal professional papers but has less stringent limitations on manuscript length and extent of graphic presentations.
- **TECHNICAL MEMORANDUM.** Scientific and technical findings that are preliminary or of specialized interest, e.g., quick release reports, working papers, and bibliographies that contain minimal annotation. Does not contain extensive analysis.
- **CONTRACTOR REPORT.** Scientific and technical findings by NASA-sponsored contractors and grantees.

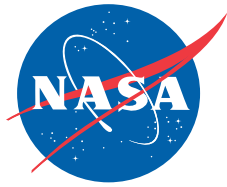
- **CONFERENCE PUBLICATION.** Collected papers from scientific and technical conferences, symposia, seminars, or other meetings sponsored or cosponsored by NASA.
- **SPECIAL PUBLICATION.** Scientific, technical, or historical information from NASA programs, projects, and missions, often concerned with subjects having substantial public interest.
- **TECHNICAL TRANSLATION.** English-language translations of foreign scientific and technical material pertinent to NASA's mission.

Specialized services also include creating custom thesauri, building customized databases, and organizing and publishing research results.

For more information about the NASA STI program, see the following:

Access the NASA STI program home page at <http://www.sti.nasa.gov>.

- E-mail your question via the Internet to help@sti.nasa.gov.
- Fax your question to the NASA STI Help Desk at (301) 621-0134.
- Phone the NASA STI Help Desk at (301) 621-0390.
- Write to:
NASA STI Help Desk
NASA Center for AeroSpace Information
7115 Standard Drive
Hanover, MD 21076-1320



Tailored Excitation for Frequency Response Measurement Applied to the X-43A Flight Vehicle

*Ethan Baumann
NASA Dryden Flight Research Center
Edwards, California*

National Aeronautics and
Space Administration

Dryden Flight Research Center
Edwards, California 93523-0273

January 2007

NOTICE

Use of trade names or names of manufacturers in this document does not constitute an official endorsement of such products or manufacturers, either expressed or implied, by the National Aeronautics and Space Administration.

Available from:

NASA Center for AeroSpace Information
7115 Standard Drive
Hanover, MD 21076-1320
(301) 621-0390

ABSTRACT

An important aspect of any flight research project is assessing aircraft stability and flight control performance. In some programs this assessment is accomplished through the estimation of the in-flight vehicle frequency response. This estimation has traditionally been a lengthy task requiring separate swept sine inputs for each control axis at a constant flight condition. Hypersonic vehicles spend little time at any specific flight condition while they are decelerating. Accordingly, it is difficult to use traditional methods to calculate the vehicle frequency response and stability margins for this class of vehicle. A technique has been previously developed to significantly reduce the duration of the excitation input by tailoring the input to excite only the frequency range of interest. Reductions in test time were achieved by simultaneously applying tailored excitation signals to multiple control loops, allowing a quick estimate of the frequency response of a particular aircraft. This report discusses the flight results obtained from applying a tailored excitation input to the X-43A longitudinal and lateral-directional control loops during the second and third flights. The frequency responses and stability margins obtained from flight data are compared with preflight predictions.

NOMENCLATURE

6-DOF	six-degree-of-freedom
AMW	all-moving wing
DFRC	NASA Dryden Flight Research Center
dB	decibels
FFT	Fast Fourier Transform
GNC	guidance, navigation, and controls
G_{xx}	input autospectral density
G_{xy}	cross-spectral density
G_{yy}	output autospectral density
HXLV	Hyper-X Launch Vehicle
HXRV	Hyper-X Research Vehicle
IPT	integrated product team
K_m	scale factor of m^{th} input
k	discrete frequency variable
LaRC	NASA Langley Research Center
MIMO	multiple-input/multiple-output
n_f	number of frequencies
PID	parameter identification
R_{max}	maximum desired input rate

t	time
U_m	final m^{th} input signal
u_m	intermediate m^{th} input signal
\dot{u}	input signal derivative
γ_{xy}^2	magnitude squared coherence
λ_m	wavelength of m^{th} signal
Φ_m	phase shifting of m^{th} signal

INTRODUCTION

When flight-testing a new vehicle such as the X-43A it is desirable to estimate the in-flight frequency response and stability margins of the vehicle. This information has traditionally been used to clear an aircraft to a new portion of the flight envelope and to validate preflight models. In addition, a multiple-input/multiple-output (MIMO) system analysis can yield valuable information concerning the robustness of the vehicle control system. For the X-43A, also known as the Hyper-X Research Vehicle (HXRV), this information was desired for post-flight analysis and to aid in model validation.

A shortcoming in performing in-flight frequency response analysis has been the long duration of the excitation signal required to obtain this information. Traditionally, a swept sinusoid is used as the excitation signal. The swept sinusoid is often input by the pilot and requires a relatively long dwell time at a given flight condition (ref. 1). The HXRV rapidly descends in altitude and in Mach number following the completion of the scramjet engine test. This rapid descent made it desirable to utilize an excitation method that would quickly excite the control loops, before the vehicle had moved on to a significantly different flight condition.

The use of tailored excitation input signals provides a measurement of the system frequency response over a specified range of frequencies. The duration of the input signal can be minimized by utilizing only the frequency range required for stability margin verification. Additionally, the simultaneous application of the excitation signal to all of the vehicle control inputs allows for short-duration tests. These simultaneous inputs consist of uncorrelated frequency components. By using phase shifting as described by Schroeder (ref. 2), it is possible to minimize the magnitude of these tailored excitation signals. This technique has been shown to be superior to traditional methods (ref. 3).

Simultaneous tailored inputs allow for rapid estimation of the vehicle frequency response in each control loop. Chirp-Z transformation algorithms can be used to extract the response at the specifically excited frequencies. A Fast Fourier Transform (FFT) can also be used to extract frequency response information provided the individual frequencies of the input signal sufficiently approximate a continuous frequency range. In addition, the singular values of the MIMO system can be estimated. The methodology and feasibility of using tailored excitation input signals for frequency response estimation were explored in a simulation environment by Bosworth and Burken (ref. 4). The work done by Bosworth and Burken applied only to the longitudinal axis of

the X-31A. A similar technique has been applied to the lateral-directional axes of the NASA F-15 ACTIVE research aircraft for aerodynamic parameter estimation (ref. 5). The tailored inputs used for the X-43A simultaneously excited the longitudinal and lateral-directional axes in flight, which is the first time this simultaneous excitation has been attempted at the NASA Dryden Flight Research Center (DFRC), Edwards, California.

This report discusses the in-flight application of simultaneous tailored input excitation signals to the HXRV. The flight-data-derived frequency response and high-frequency stability margin measurements are presented, along with a comparison with linear model predictions.

PROJECT DESCRIPTION

The Hyper-X program was an experimental flight research program intended to demonstrate advanced hypersonic technologies (ref. 6). The primary research objective was to flight-test an airframe-integrated scramjet engine and validate the vehicle design tools. Hypersonic research is intended to enable the development of high-speed airbreathing technologies, which could be used in future high-speed aircraft and reusable launch vehicles. The NASA Langley Research Center (LaRC), Hampton, Virginia was the Hyper-X program lead, and NASA DFRC led the flight-test effort. Each flight test consisted of two vehicles: a launch vehicle and a research vehicle. The Hyper-X Launch Vehicle (HXLV) was provided by Orbital Sciences Corporation of Chandler, Arizona. An industry team consisting of Alliant Technosystems, Inc., GASL Division (Tullahoma, Tennessee) and Boeing Phantom Works (Seal Beach, California) constructed the HXRV.

HYPER-X RESEARCH VEHICLE DESCRIPTION

As shown in figure 1, the HXRV was an unmanned autonomous vehicle that measured approximately 12 ft long and 5 ft wide, and weighed approximately 3000 lb. The scramjet engine was attached to the underside of the HXRV. A cowl door on the leading edge of the engine controlled airflow through the engine. The HXRV had four control surface effectors: a left and right all-moving wing (AMW) and twin rudders. The rudders moved symmetrically, and the AMWs moved symmetrically and differentially for pitch and roll control. Symmetric AMW deflection is defined as elevator deflection, and differential AMW deflection is defined as aileron deflection.

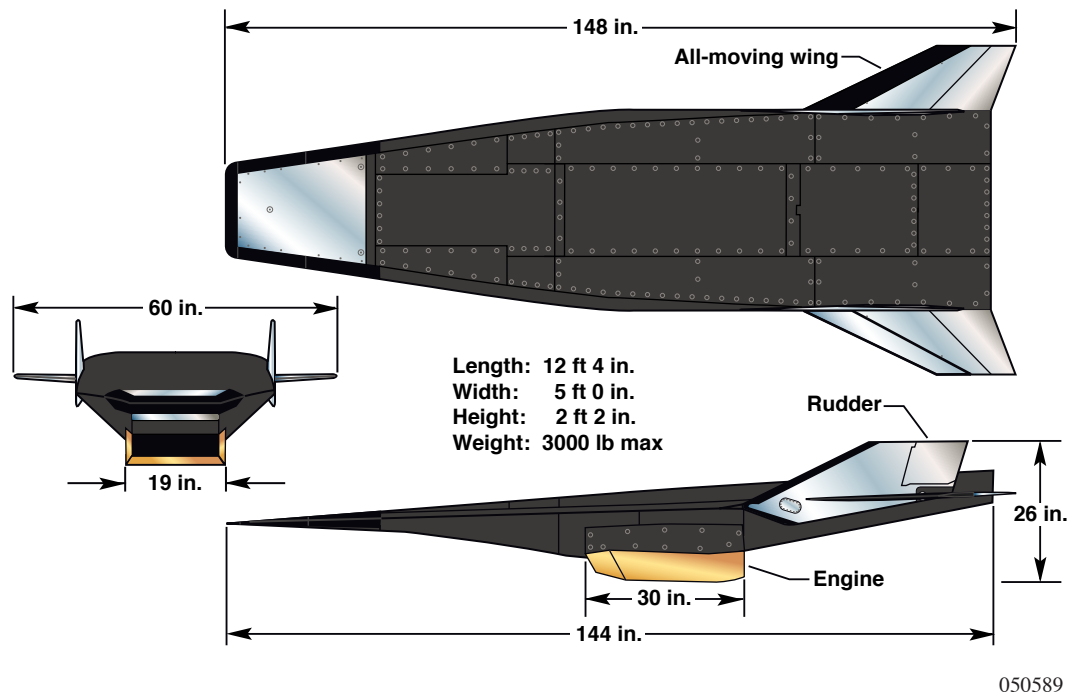


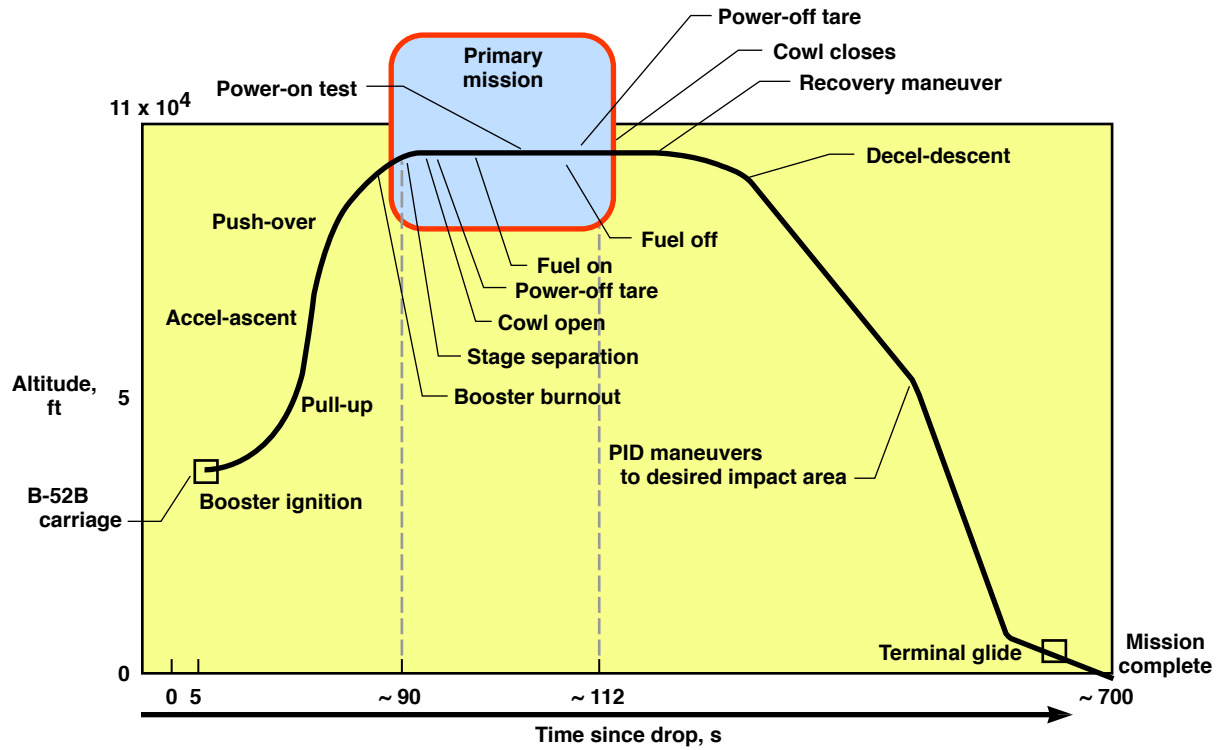
Figure 1. Hyper-X Research Vehicle three-view.

HYPER-X RESEARCH VEHICLE FLIGHT TEST

Three HXRVs were built for the Hyper-X program. Two of the vehicles were intended for missions at Mach 7, and one vehicle was intended for a mission at Mach 10. The HXRVs collectively received the designation of X-43A. All three vehicles have the same outer mold line; the primary difference among the vehicles is the internal engine flowpaths. Flight 1 was intended to reach Mach 7 and was attempted on June 2, 2001. The HXLV lost control shortly after launch, resulting in the loss of both the HXLV and HXRV (ref. 7). During Flight 2, flown to Mach 6.8 on March 27, 2004, the HXRV successfully demonstrated the in-flight operation of the scramjet (ref. 8). All of the goals for that mission were achieved, including positive acceleration of the vehicle by the scramjet. The third and final flight was flown to Mach 9.6 on November 16, 2004 (ref. 9). During both successful missions, the HXRV was in controlled autonomous flight from the point of separation to the splashdown in the Pacific Ocean.

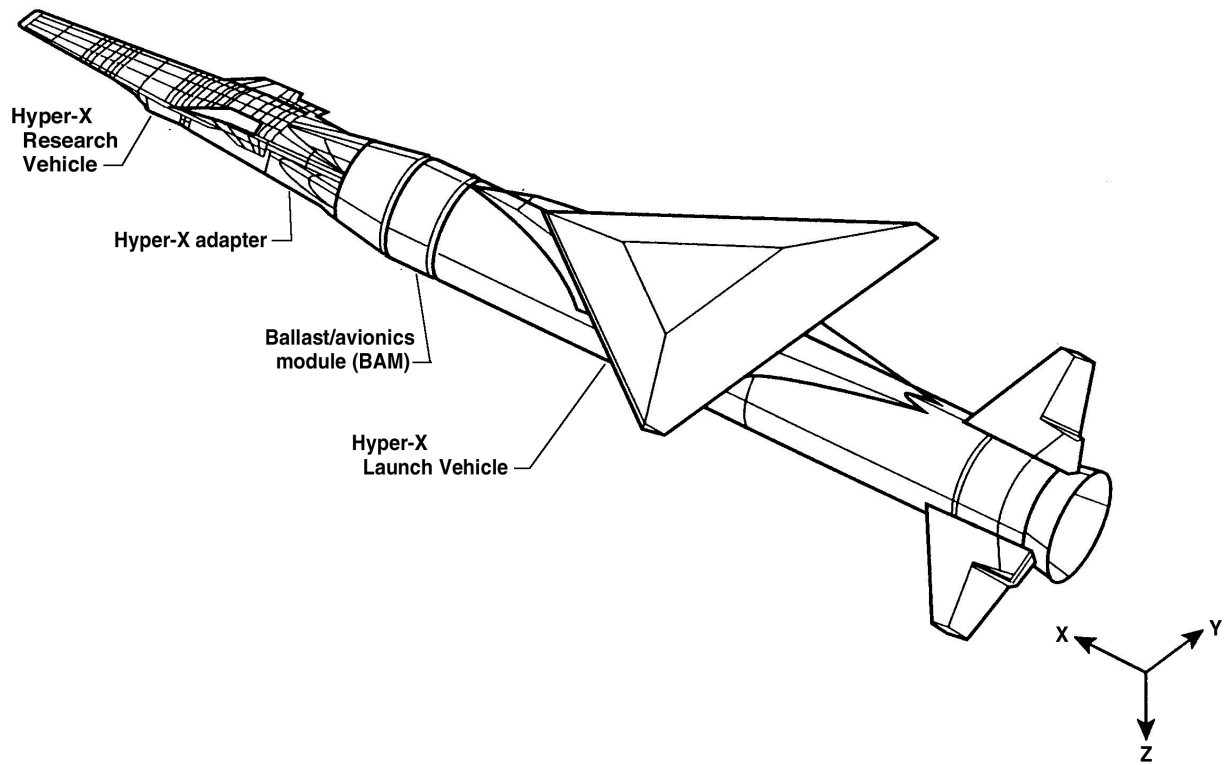
HYPER-X RESEARCH VEHICLE MISSION DESCRIPTION

The HXRV mission timelines were similar for Flight 2 and Flight 3. The principal difference between the two flights is the higher Mach number attained during Flight 3, which resulted in a correspondingly longer descent trajectory. Figure 2 shows an overview of Flight 3. The launch, experiment, and descent portions of the mission were conducted off the coast of southern California. The HXRV was boosted to the test condition by the HXLV. The HXRV was connected to the HXLV by an adapter module. The entire configuration, known as the X-43A stack and shown in figure 3, was carried under the wing of the NASA DFRC NB-52B, ship number 008.



050590

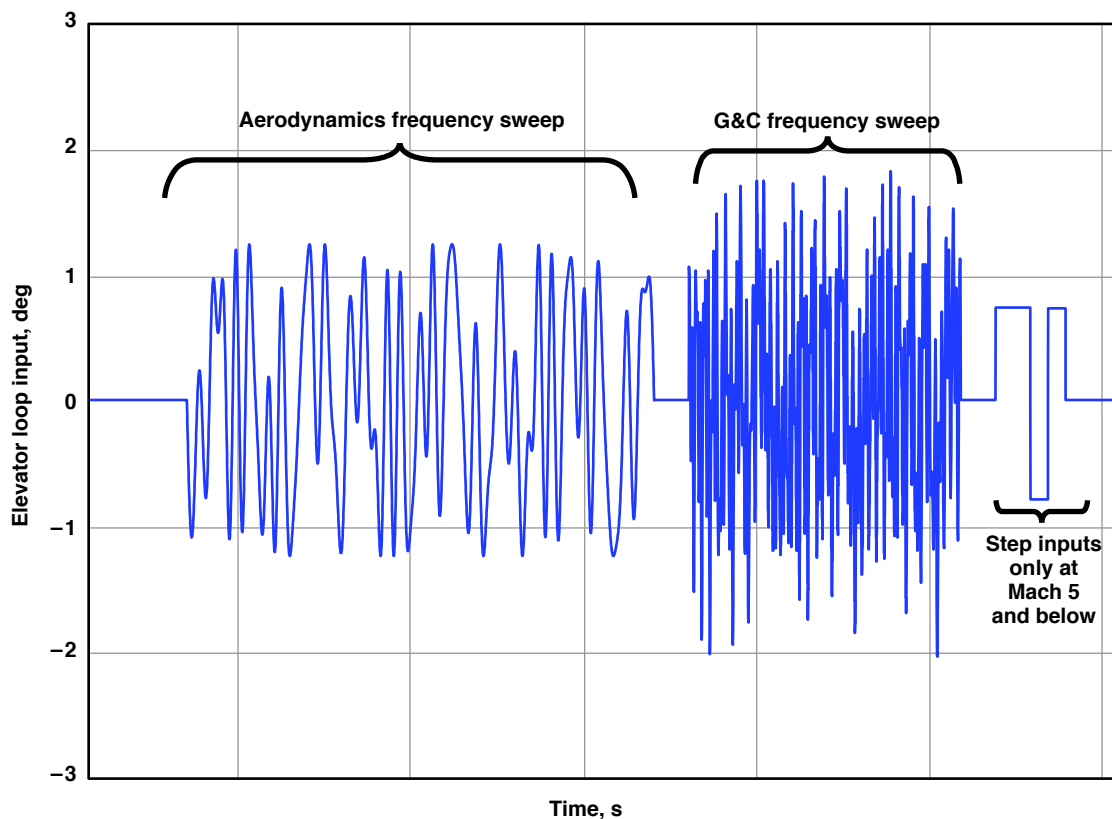
Figure 2. Hyper-X Research Vehicle Flight 3 overview.



050591

Figure 3. The X-43A stack configuration.

For both missions, the HXLV propelled the X-43A stack to a separation altitude of approximately 100 000 ft and a dynamic pressure of approximately 1000 psf. The HXRV separated at Mach 6.9 during Flight 2 and at Mach 9.7 during Flight 3. Several seconds after separation, the primary experiment of the scramjet engine test was conducted. The primary mission portion lasted approximately 45 s for Flight 2 and 30 s for Flight 3. Following the primary mission, an unpowered trajectory was flown to a splashdown into the Pacific Ocean. During the descent, a series of parameter identification (PID) maneuvers were performed at every integer Mach number down to Mach 2. These maneuvers began at Mach 5 during Flight 2 and at Mach 8 during Flight 3. The HXRV was constantly decelerating throughout the PID maneuvers, so the Mach number was not constant. The PID maneuvers consisted of control surface inputs designed by the aerodynamics Integrated Product Team (IPT) (ref. 10) and guidance, navigation, and controls (GNC) IPT. Figure 4 shows the Mach 5 PID input set for the elevator loop from Flight 3. The aerodynamics IPT's inputs were intended to characterize the rigid body aircraft characteristics and consisted of step inputs for both Flights, and frequency sweeps for Flight 3. The aerodynamics IPT's input set occurred at the beginning and end of the PID maneuver set, and consisted of inputs that excited the vehicle over a lower frequency range than did the GNC IPT's inputs. The GNC IPT's inputs consisted of tailored excitation inputs to the control loops intended to characterize the vehicle open-loop frequency response. All inputs were added directly to the control loop commands generated by the flight control laws.



050592

Figure 4. Mach 5 elevator loop parameter identification maneuver from Flight 3.

INPUT EXCITATION SIGNAL

The simultaneous tailored input excitation signals used on the HXRV consisted of a series of summed sine waves. A summed sine wave has the advantage of reducing the excitation time when compared with a traditional swept sine wave. The method used to generate the input signals generally follows that described by Bosworth and Burken (ref. 4), but a modification was made to the method to prevent control surface rate limiting.

The simultaneous tailored excitation signals were generated following the method described by Bosworth and Burken (ref. 4). The frequency range was selected such that the preflight gain and phase crossover frequency predictions for the HXRV were within the selected range. Once the frequency range had been selected, 35 distinct frequencies for each control loop were calculated. Table 1 details the input frequencies for each control loop. The method for selecting the input frequencies resulted in a smaller spacing between frequencies toward the upper end of the range. This spacing resulted in the input sines being sufficiently close enough in frequency range for the FFT method to work well above approximately 0.9 Hz.

Equations (1) through (4) below were used to construct the input excitation signals.

The input excitation signal for the m^{th} input is

$$u_m = \left[\sum_{n=1}^{nf/3} \sin(\lambda_m(n)t + \Phi_m(n)) \right] \quad (1)$$

where $\lambda_m(n)$ is the wavelength of each frequency and $\Phi_m(n)$ is the phase shifting used to reduce the peak factor of the excitation while maintaining the same frequency content (ref. 2).

For the HXRV, each of the input signals was scaled to limit the control surface input. This scaling was necessary to prevent actuator rate limiting so as to retain actuator margin for maneuvering. A value of 50 deg/s was used as the maximum allowable rate limit when designing the inputs for the HXRV. This value was chosen to keep the commanded surface position rate change for each control surface within the actuator limit of approximately 100 deg/s, while retaining an adequate maneuvering margin.

The derivative of each input signal is calculated to find the maximum rate of change of the input signal:

$$\dot{u}_m = \left[\sum_{n=1}^{nf/3} \lambda_m \cos(\lambda_m(n)t + \Phi_m(n)) \right] \quad (2)$$

Table 1. Excitation input frequencies.

Elevator	Aileron	Rudder
frequency, Hz		
0.25	0.19	0.32
0.45	0.38	0.51
0.64	0.57	0.70
0.83	0.76	0.89
1.02	0.95	1.08
1.21	1.15	1.27
1.40	1.34	1.46
1.59	1.53	1.66
1.78	1.72	1.85
1.97	1.91	2.04
2.16	2.10	2.23
2.36	2.29	2.42
2.55	2.48	2.61
2.74	2.67	2.80
2.93	2.86	2.99
3.12	3.06	3.18
3.31	3.25	3.37
3.50	3.44	3.56
3.69	3.63	3.76
3.88	3.82	3.95
4.07	4.01	4.14
4.26	4.20	4.33
4.46	4.39	4.52
4.65	4.58	4.71
4.84	4.77	4.90
5.03	4.97	5.09
5.22	5.16	5.28
5.41	5.35	5.47
5.60	5.54	5.67
5.79	5.73	5.86
5.98	5.92	6.05
6.17	6.11	6.24
6.37	6.30	6.43
6.56	6.49	6.62
6.75	6.68	6.81

A scale factor (K_m) is then found by dividing the maximum desired rate (R_{\max}) by the maximum value of the derivative of the input signal:

$$K_m = \frac{R_{\max}}{\max(\dot{u}_m)} \quad (3)$$

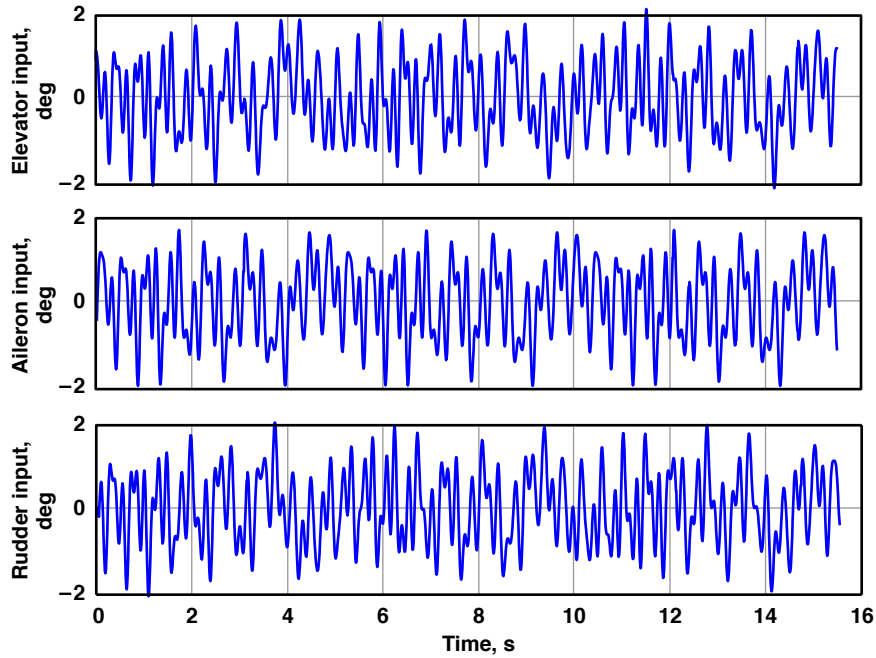
The input signals are then scaled by K_m to minimize the control surface rate change:

$$U_m = K_m u_m \quad (4)$$

The end result is three input signals that are now uncorrelated, periodic, and appropriately scaled.

INPUT SIGNAL USED FOR X-43A

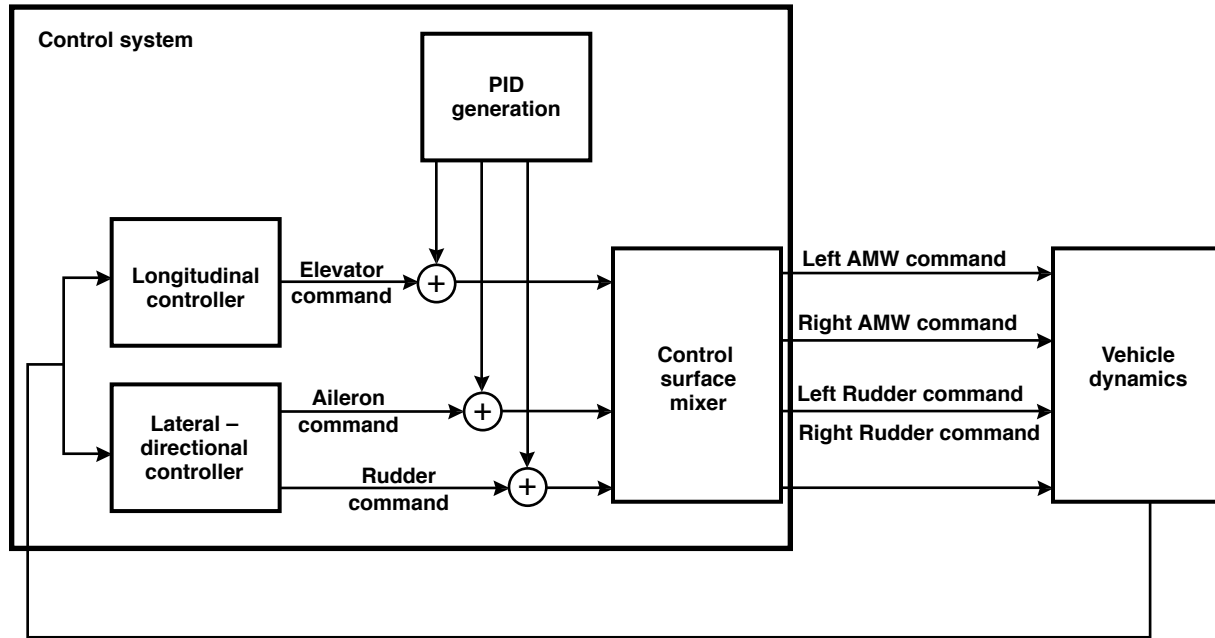
The excitation inputs were embedded in the X-43A flight control laws and were activated during the descent PID maneuvers. Table 1 details the frequencies used for the elevator, aileron, and rudder loop excitation frequencies. Figure 5 shows the time history trace for each of the three inputs. The same inputs were used at each PID maneuver set during the descent.



050557

Figure 5. Hyper-X Research Vehicle tailored excitation signal time histories.

Figure 6 is a block diagram showing how the excitation signals are applied to each control axis. The inputs are added to the commands generated by the flight control system. The flight control system consists of a longitudinal and lateral-directional controller (ref. 11). The open-loop transfer function is then calculated between the tailored excitation signal and the output of the longitudinal and lateral-directional controllers. Both the input and output data for the transfer function are obtained as 100-Hz signals.



050558

Figure 6. Block diagram detailing the application of the tailored excitation input signals to the Hyper-X Research Vehicle.

RESPONSE ESTIMATION

Both Chirp-Z and Fast Fourier transforms were applied to the HXRV flight data to calculate the in-flight frequency responses. A Chirp-Z transform can be used to match the input and output frequencies. Only those frequencies present in the input are examined in a Chirp-Z transform. The FFT method is a computationally efficient way to implement the Discrete Fourier Transform, which is used to transform discrete data from the time domain to the frequency domain.

The FFT method also provides an indication of the quality of the input-output relationship. This quality is determined by examining the magnitude squared coherence function shown in equation (5).

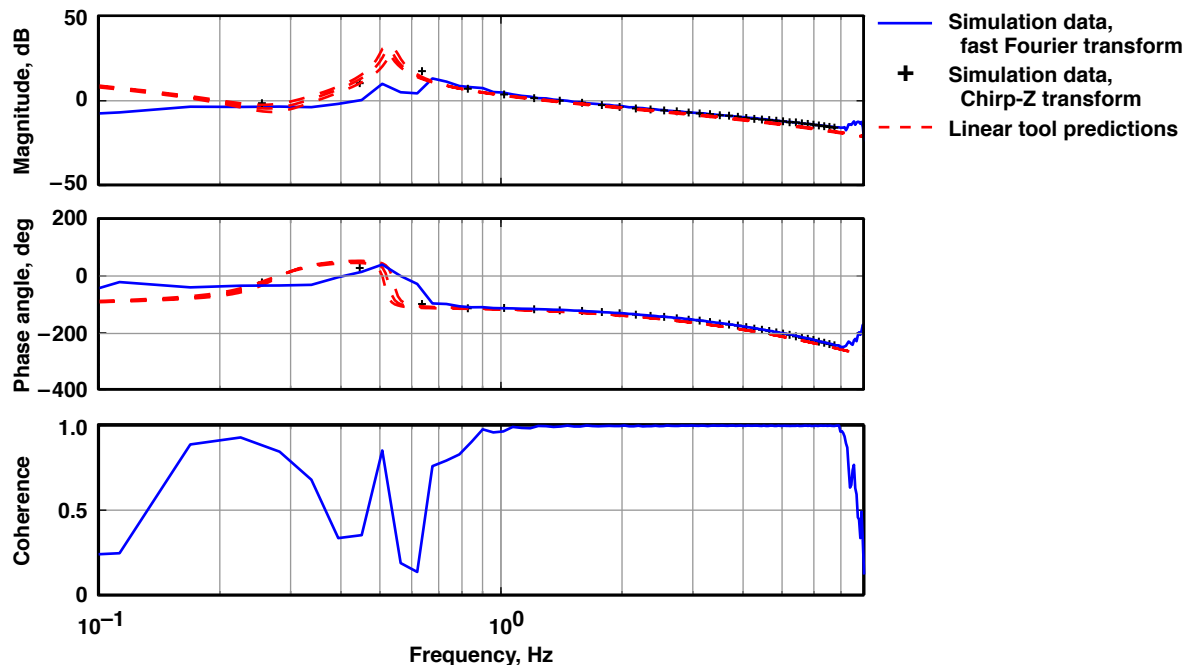
$$\gamma_{xy}^2(k) = \frac{|G_{xy}(k)|^2}{|G_{xx}(k)||G_{yy}(k)|} \quad (5)$$

A linear, noise-free system would yield a coherence of 1. System nonlinearities, input and output noise, and secondary inputs would produce a coherence below 1. For the purposes of this report, a coherence value of 0.8 indicates an acceptable response measurement.

LINEAR MODEL AND SIX-DEGREE-OF-FREEDOM NONLINEAR SIMULATION

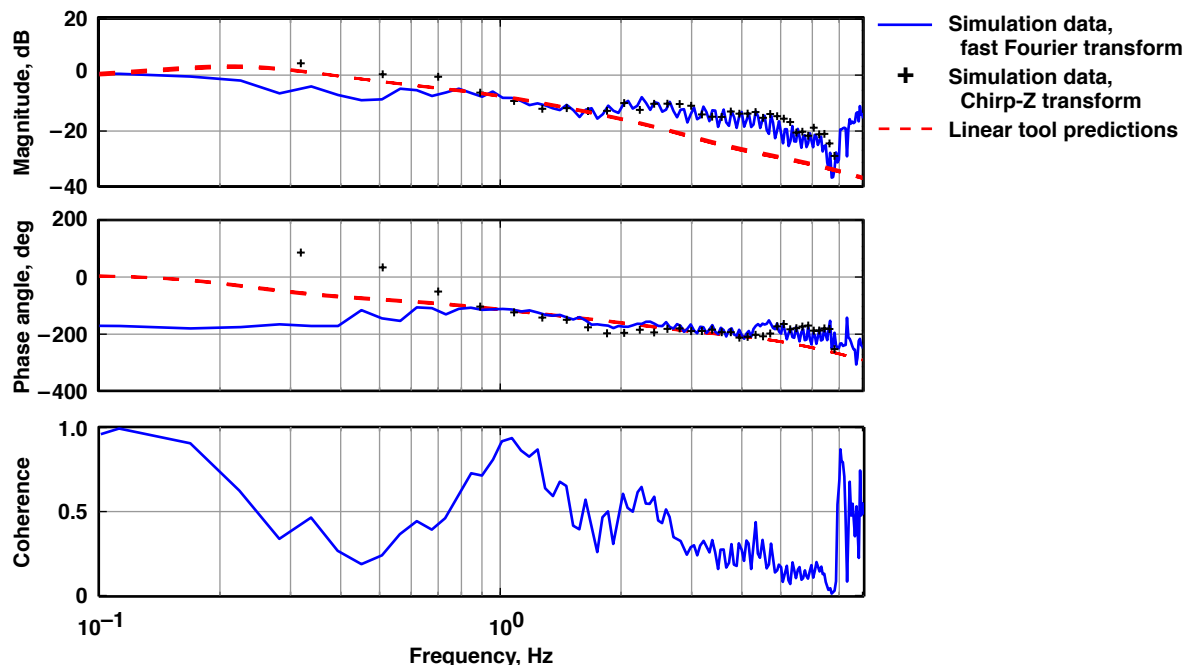
The Hyper-X program developed a high-fidelity six-degree-of-freedom (6-DOF) nonlinear simulation model of the X-43A along with a simplified linear model used for control law design and analysis. The 6-DOF simulation was based on the standard DFRC simulation architecture (ref. 12) and contained detailed subsystem models of the flight control system, vehicle aerodynamics, actuators, mass properties, engine, and sensors. The linear model was constructed in MATLAB® and Simulink® (both registered trademarks of The MathWorks, Inc., Natick, Massachusetts) and contained linearized versions of these subsystems.

The tailored input excitations were used in the nonlinear simulation as part of the frequency response comparison with the linear analysis tool. Figures 7 and 8 show sample elevator and rudder loop comparisons for the Mach 5 PID frequency response predictions for Flight 2. The FFT and Chirp-Z-derived frequency responses are shown compared with linear model predictions at representative flight conditions; the start, mean, and end flight conditions during the GNC portion of the PID maneuvers. The aileron loop comparison was similar to that of the elevator loop. The elevator and aileron loop results of the simulation and linear models were found to be in excellent agreement and were used prior to Flight 2 to predict the in-flight performance of the tailored excitation input signals. The rudder loop results showed discrepancies with the simulation results, which are discussed in detail in the following section.



050559

Figure 7. Comparison of elevator frequency responses for the Flight 2 Mach 5 parameter identification maneuver from the six-degree-of-freedom simulation and the linear analysis tool.



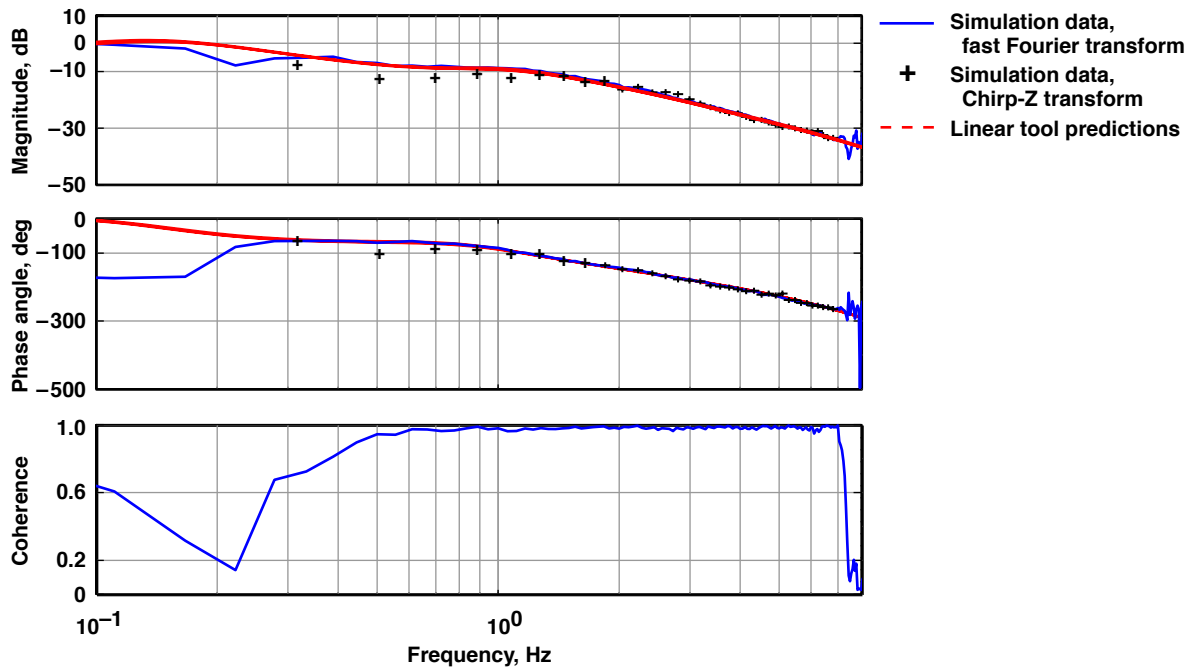
050560

Figure 8. Comparison of rudder frequency responses for the Flight 2 Mach 5 parameter identification maneuver from the six-degree-of-freedom simulation and the linear analysis tool.

PROBLEMS IDENTIFIED PRIOR TO FLIGHT

A few months prior to Flight 2, simulation testing uncovered several problems with the tailored excitation signals. Rudder loop frequency response values generated from simulation data showed very poor matches with the linear model. In addition, the coherence value for the rudder loop was below acceptable levels. The problem was discovered too late to implement a solution for Flight 2, especially considering that the descent portion of the mission was of secondary importance. Data from Flight 2, presented below, also showed poor rudder loop frequency responses.

Shortly after Flight 2, a number of approaches were investigated to improve the rudder loop frequency response results. The most effective approach was to decouple the rudder and aileron excitations. Simulation results indicated that this modification produced good comparisons between the linear analysis tools and 6-DOF simulation for the rudder loop, as shown in figure 9. This approach was adopted for Flight 3, resulting in the rudder and aileron control loop inputs being applied at alternating Mach numbers. The improvement in the rudder loop comparisons when applied without the aileron loop inputs indicates a correlation between the rudder and aileron loop responses that is not understood at this time.



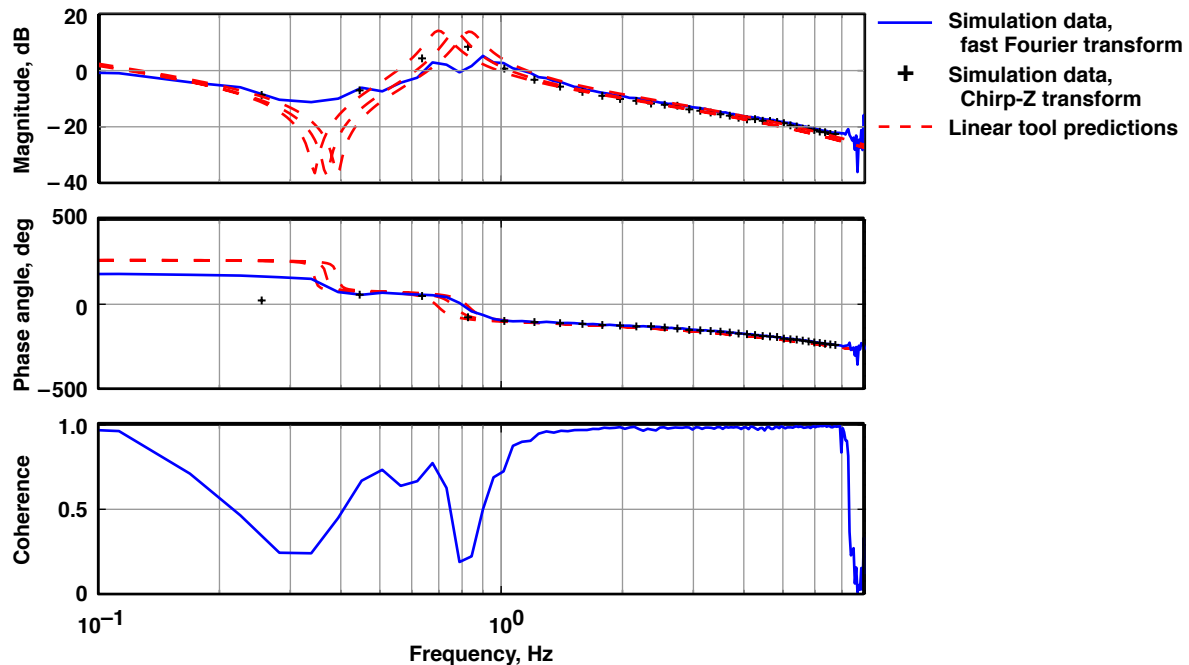
050561

Figure 9. Rudder loop frequency response comparison between six-degree-of-freedom simulation and linear analysis tools when input decoupled from aileron loop for the Flight 3 Mach 4 parameter identification maneuver.

Another possible explanation for the poor rudder loop comparisons is that the magnitude of the rudder excitation was insufficient to move beyond the rudder actuation system nonlinearities. The excitation input magnitude for the rudder was increased in the simulation with mixed results. The response improved slightly, but was still inadequate.

As a result of the poor rudder frequency response estimation, MIMO analysis was not conducted. A MIMO analysis requires valid transfer function values from all control axes. The poor characteristics of the rudder loop frequency response data precluded attempting any MIMO analysis on Flight 2 data. In addition, Flight 3 did not simultaneously excite the aileron and rudder loops at the same flight condition. Valid aileron and rudder frequency responses were never obtained at the same flight condition, thereby precluding any flight-data-derived MIMO stability analysis for the X-43A for either flight.

The simulation comparisons with the linear analysis predictions displayed another problem with the input signals. The elevator frequency responses for the Mach 2 PID did not match linear predictions as well as did those at the higher Mach numbers. Figure 10 shows the Flight 2 elevator loop simulation and linear analysis comparison for the Mach 2 PID. The excitation signals occur near the end of the PID maneuver set, so they finished near or in the transonic regime. The longitudinal aerodynamics of the vehicle change rapidly as the vehicle maneuvers through the transonic regime; the poor matches are not unexpected since the linear analysis results are at a specific flight condition.



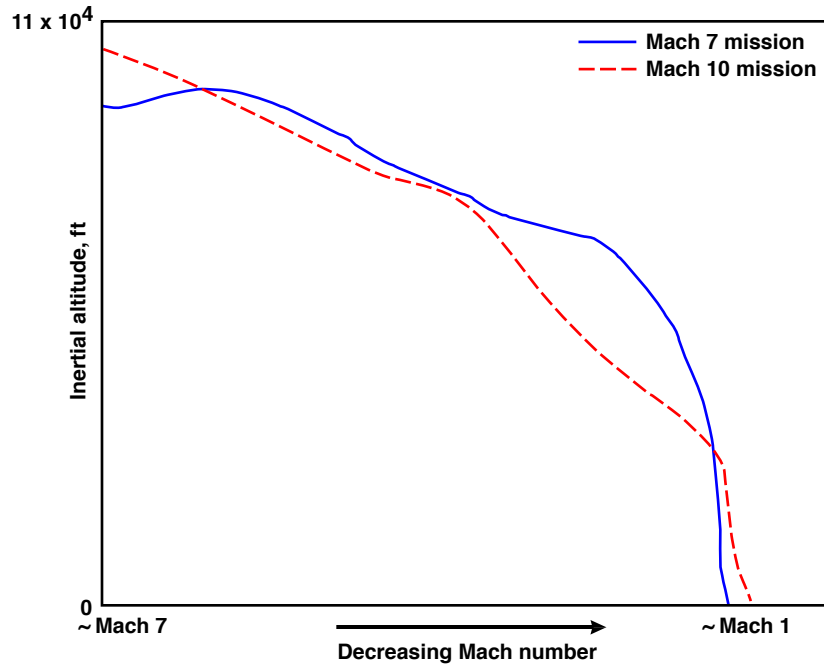
050562

Figure 10. Comparison of elevator frequency responses for the Flight 2 Mach 2 parameter identification maneuver from the six-degree-of-freedom simulation and the linear analysis tool.

FLIGHT RESULTS

For both Flights 2 and 3, the HXRV achieved scramjet operation and successfully flew an unpowered descent into the Pacific Ocean. Figure 11 shows the altitude profile for the two flights. As can be seen, the two flights flew different descent profiles in the common Mach regions. In addition, the control system used for Flights 2 and 3 utilized different gain schedules. These differences render direct comparisons between the two flights impossible. It is possible, however, to examine the quality of the linear values to flight-derived frequency response comparisons between the two flights.

Flight 3 included an unusual event after the engine test that affected the vehicle flight characteristics. It is believed that air started flowing through the engine shortly after the initiation of the recovery maneuver. The cowl door had been commanded closed at the end of the engine test, and this closing had shut off the majority of the air flowing through the engine as expected. An unknown mechanism allowed significant quantities of air to flow through the vehicle shortly after the engine test. Just prior to the Mach 8 PID maneuvers, the internal engine pressures indicated a decrease in the amount of air flowing through the vehicle. The vehicle aerodynamics was significantly different with air flowing through the engine than during cowl-closed operations. The nonlinear simulation and linear analysis tools lack the capability to model air flowing through the engine during the descent. It is not known to what extent the differences between the in-flight and linear analysis values for the frequency responses and stability margins are attributable to this phenomenon.



050563

Figure 11. Post-engine-test inertial altitude comparison between Flights 2 and 3.

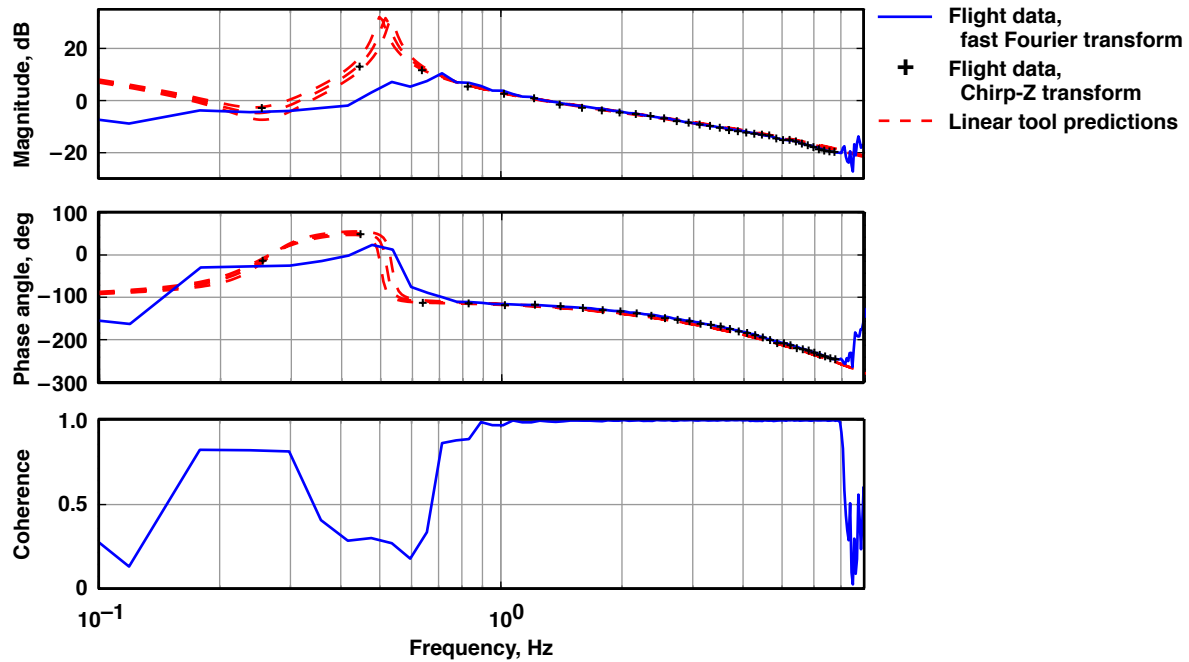
Linear analysis predictions were generated for comparison with the flight-data-derived frequency responses. Representative flight conditions at the start, mean, and end of the tailored excitation inputs were used to generate the linear analysis responses. Onboard vehicle data from each flight was used to generate the flight conditions for the linear analysis. The Mach number and dynamic pressure were estimated onboard with the inertial velocity measurements and a reference atmosphere. The angle of attack is the inertial in-flight measured angle of attack.

The high-frequency stability margins are calculated from the frequency response data by linear interpolation. The MATLAB margin function was used to perform this calculation.

The coherence values for each control loop and Mach number combination were examined. In general, the coherence values were near 1 for the elevator and aileron loops for both flights over the frequency range of interest. The rudder loop coherence was poor for Flight 2 and acceptable for Flight 3. The rudder loop frequency response measurements were found to compare well with the linear analysis predictions when the coherence value was above 0.8.

ELEVATOR LOOP RESULTS

Figure 12 shows a Bode plot comparing the elevator loop in-flight frequency response for the Mach 5 PID maneuver of Flight 2 with that of the linear models. The comparison seen in figure 12 is representative of the elevator loop frequency response comparisons for both Flights 2 and 3. The comparisons are excellent in the frequency range excited by the input signal.

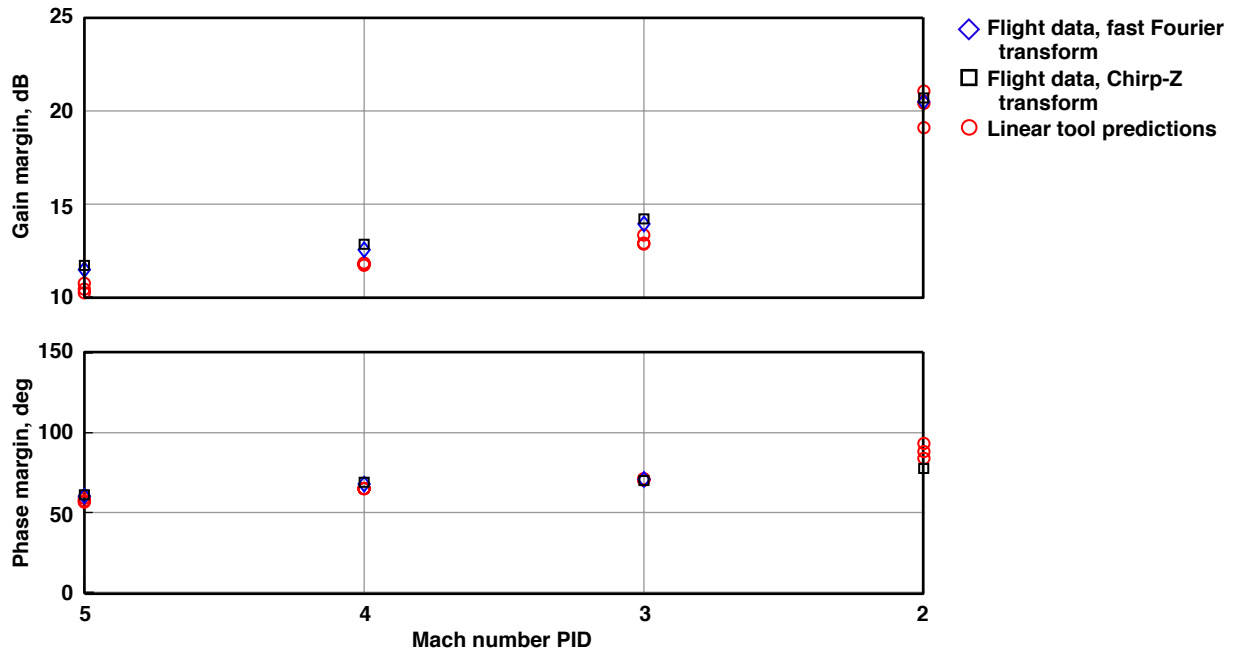


050564

Figure 12. Elevator loop frequency response comparisons for the Flight 2 Mach 5 parameter identification maneuver.

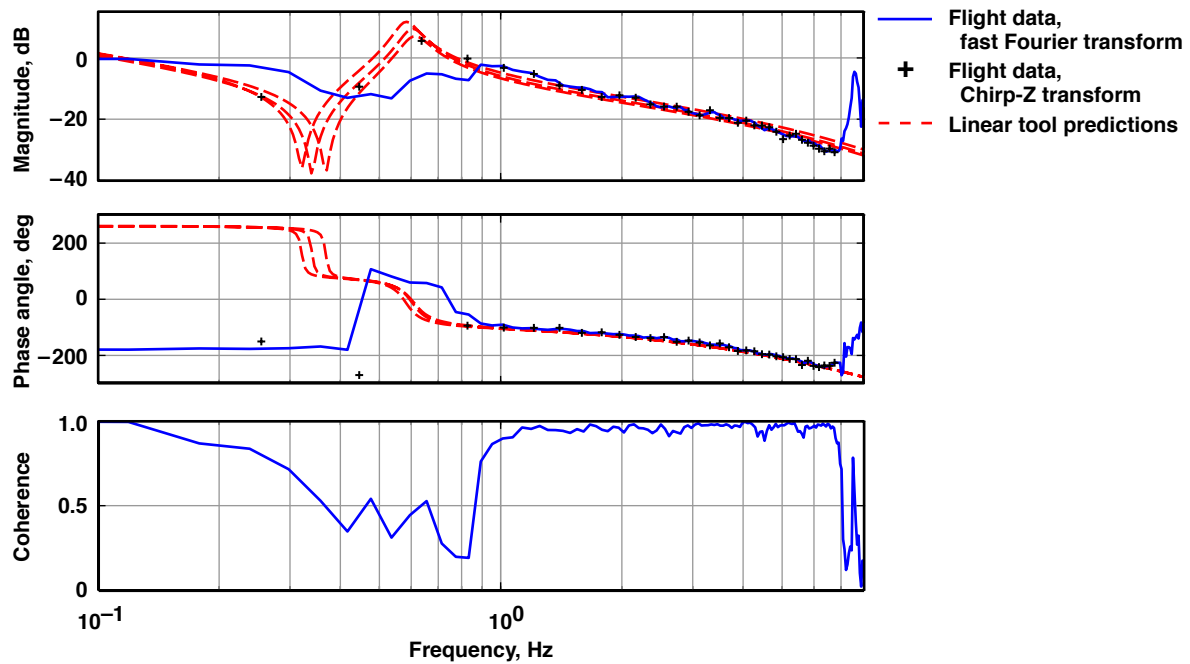
The elevator loop stability margin values for the HXRV during Flight 2 can be seen in figure 13. The gain and phase margin measurements are generally within 1.6 dB and 5 deg of the linear model predictions. The exception is the phase margin prediction for the Mach 2 PID maneuver where the phase margin determined by the Chirp-Z method is 6 to 16 deg different from the linear analysis predictions. The elevator loop frequency response for the Mach 2 PID maneuver is shown in figure 14. The FFT method shows a lower coherence and did not return a gain crossing for phase margin calculation for the Mach 2 PID maneuver. At the corresponding flight conditions, the linear analysis predictions vary by as much as 10 deg between the start, mean, and end flight conditions. This difference indicates that the vehicle aerodynamics was changing rapidly and it is therefore not surprising that the flight-derived value is different from the linear predictions.

Figure 15 shows the stability margin values from Flight 3 for the elevator loop. The in-flight gain margin values for the Mach 8 through Mach 5 PID maneuvers are consistently higher with the greatest difference being 2.5 dB. This difference in gain margin is possibly attributable to the unmodeled effects of air flowing through the engine. The phase margin predictions at these Mach numbers match the linear predictions within 2 deg. The greatest spread in the linear analysis predictions is again seen during the Mach 2 PID maneuver set since the vehicle aerodynamics are rapidly changing as the maneuver ends in the transonic regime.



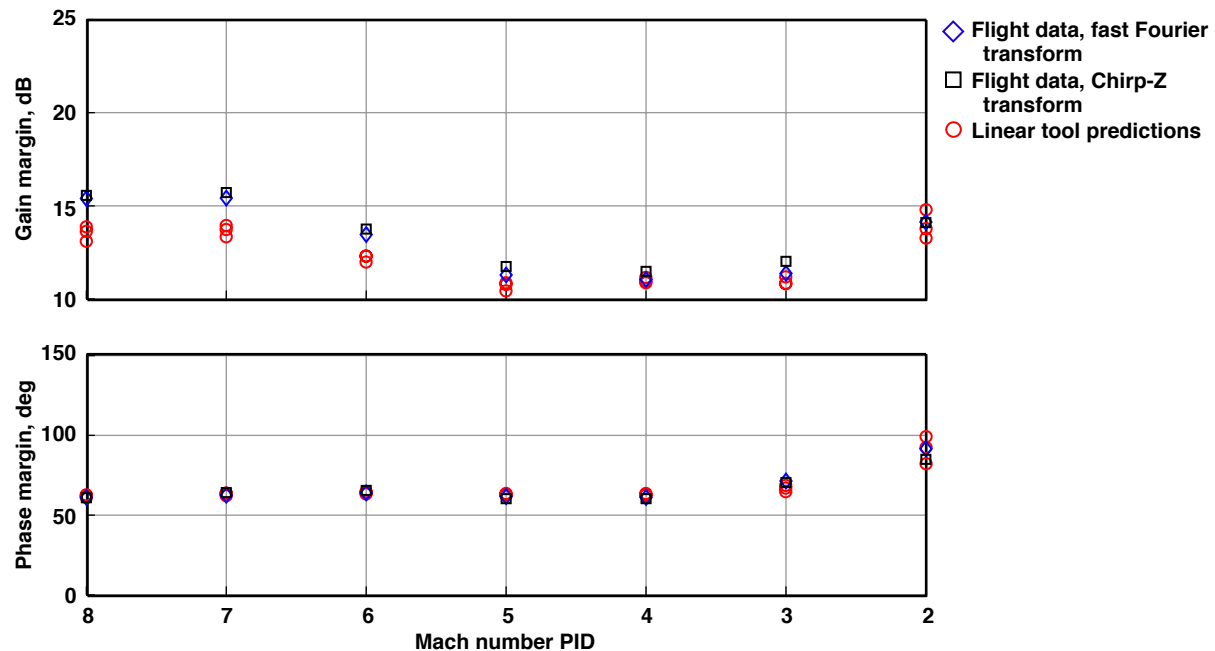
050565

Figure 13. Elevator loop stability margin estimates for Flight 2.



050566

Figure 14. Elevator loop frequency response comparisons for the Flight 2 Mach 2 parameter identification maneuver.



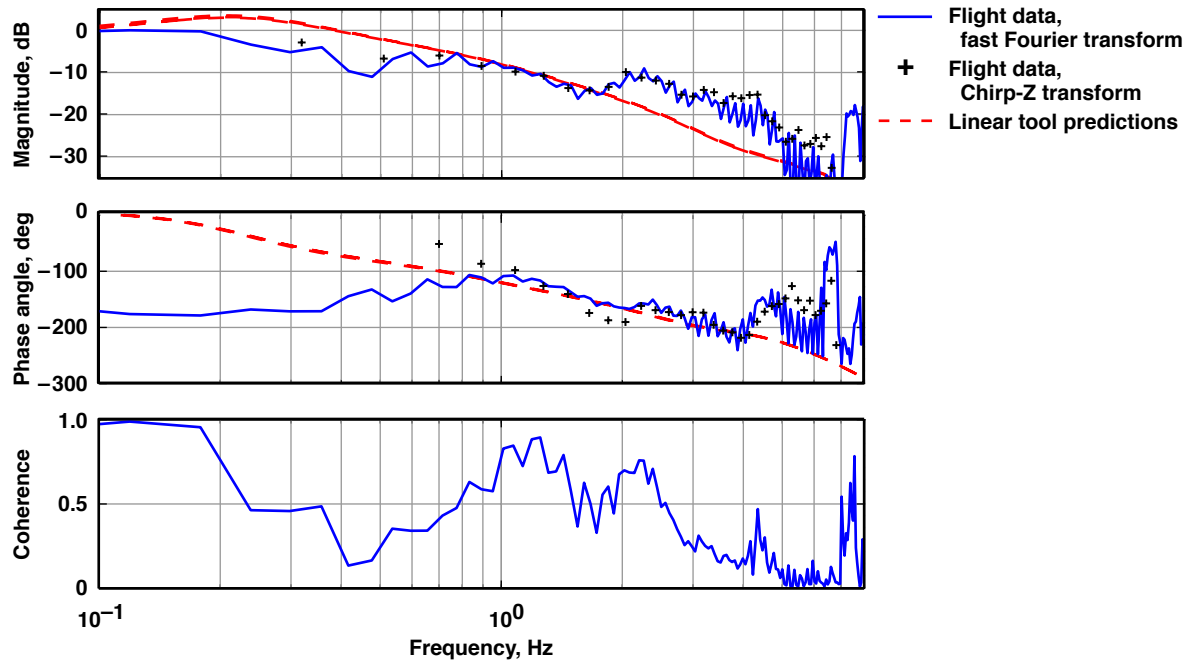
050567

Figure 15. Elevator loop stability margin estimates for Flight 3.

RUDDER LOOP RESULTS

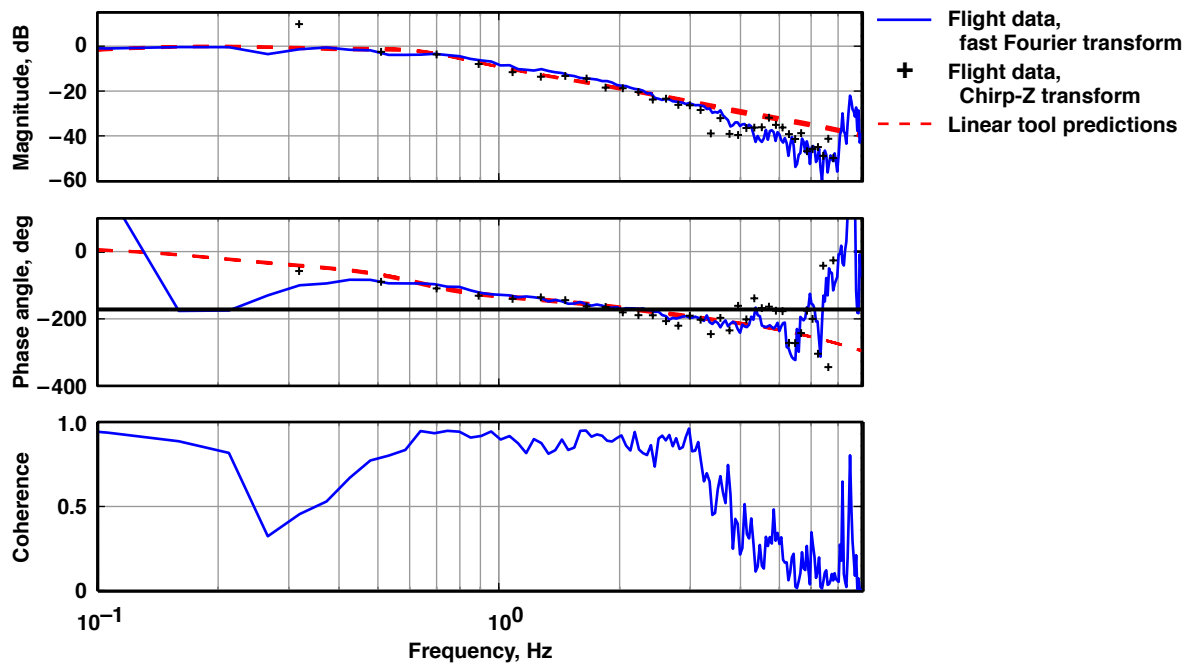
The rudder loop stability margin values for the HXRV during Flight 2 were not calculated because of the problem with obtaining an acceptable rudder loop frequency response, as discussed above. The coherence value was very poor, indicating little correlation between the input and output signals. In addition, the Chirp-Z results were not considered believable because they did not match predictions. As previously discussed, this result is believed to be because of excessive correlation between the aileron and rudder control loops. Figure 16 shows the flight-derived frequency response compared with linear model predictions for Flight 2 during the Mach 5 PID maneuver set.

As can be seen in figure 17, the rudder loop frequency responses for Flight 3 matched linear analysis predictions better than did those of Flight 2. This comparison at Mach 8 is slightly worse than for the Mach 6 and Mach 4 sets. This result is believed to be because of air flowing through the engine during the Mach 8 PID. The rudder loop frequency responses obtained from Flight 3 showed considerable improvement over those of Flight 2, however they did not compare as favorably with linear predictions as did the elevator and aileron loop responses. In particular, the FFT-derived coherence values for the rudder loop are acceptable, but not as high as for the elevator or aileron loops. Separating the aileron and rudder loop inputs for Flight 3 helped to improve the flight-derived rudder frequency response.



050568

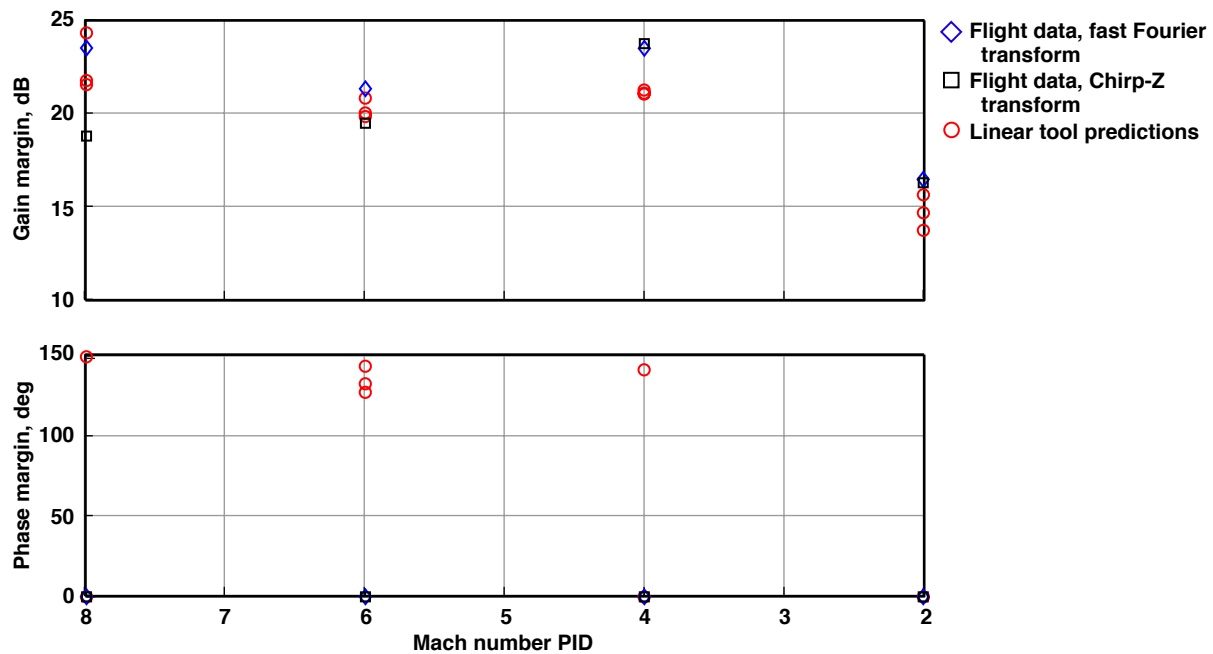
Figure 16. Rudder loop frequency response comparisons for the Flight 2 Mach 5 parameter identification maneuver.



050569

Figure 17. Rudder loop frequency response comparisons for the Flight 3 Mach 8 parameter identification maneuver.

The rudder loop stability margin comparisons for Flight 3 are presented in figure 18. The gain margin predictions are generally within 2.5 dB of the flight-derived values. The largest gain margin difference of nearly 6.0 dB was seen during the Mach 8 PID, which is when air was believed to be flowing through the engine. An infinite rudder loop phase margin was measured in flight because no in-flight gain crossover frequency was identified since the crossover frequency was generally at the lower end of the frequency range used to generate the tailored excitation input signals.



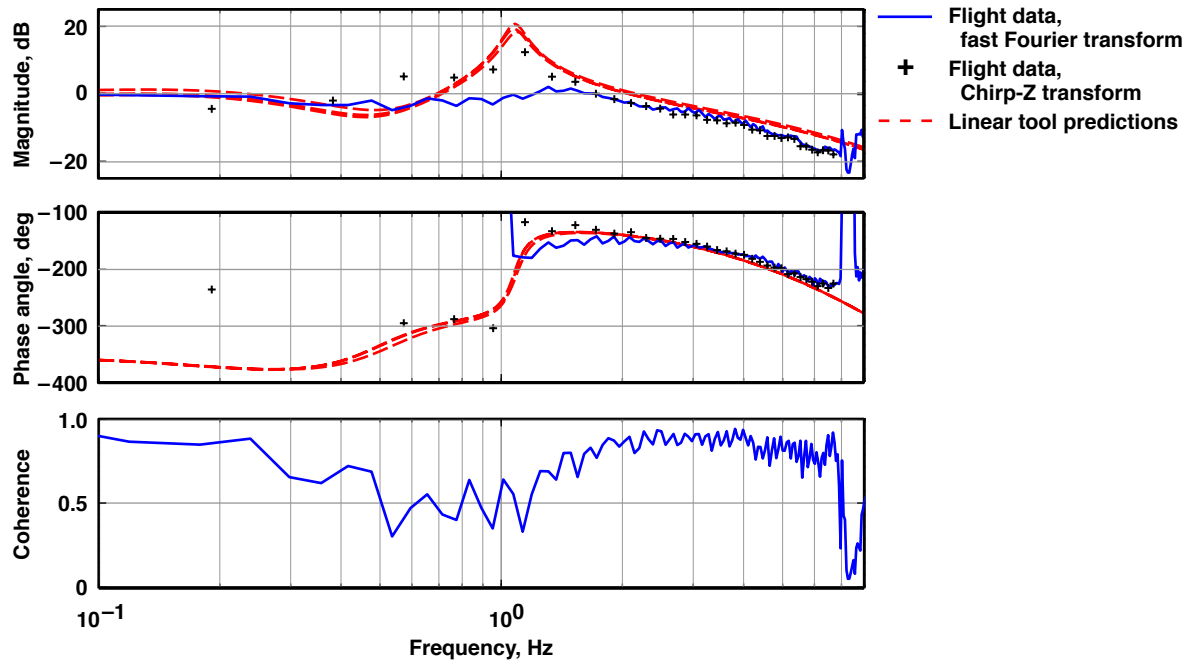
050570

Figure 18. Rudder loop stability margin estimates for Flight 3.

AILERON LOOP RESULTS

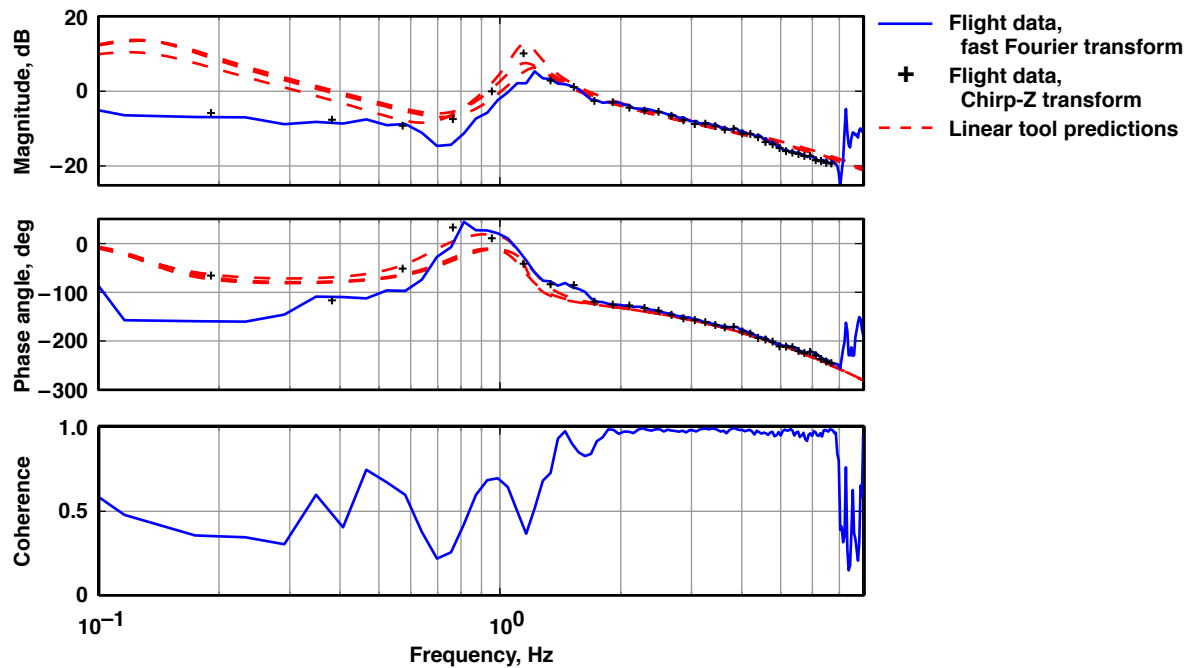
Figure 19 shows a sample aileron loop frequency response for Flight 2. This response for the Mach 2 PID maneuver showed the lowest coherence and worst comparison with linear analysis predictions. As discussed above, this result is believed to be at least partially attributable to correlation between the rudder and aileron loops. For the Mach 2 comparison only, a shift in the gain response is seen between the in-flight frequency responses and those predicted by the linear analysis tools. This shift in the gain response is possibly indicative of less aileron loop control power at this flight condition than predicted.

The aileron loop frequency responses for Flight 3 are qualitatively similar to those of Flight 2, with slightly better coherence values. The slightly better aileron loop coherence values seen in the Flight 3 data are possibly because of the aileron and rudder loops not being simultaneously excited. Figure 20 shows a representative Bode plot detailing the Mach 3 PID frequency response comparison with the linear model predictions for Flight 3.



050571

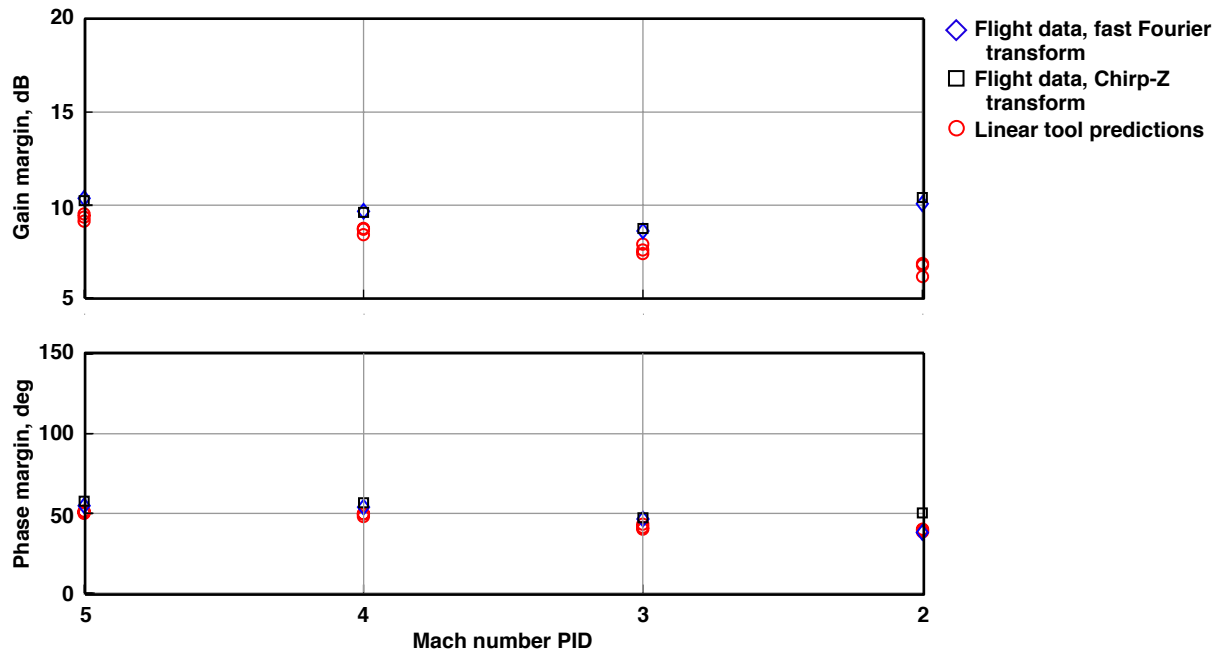
Figure 19. Aileron loop frequency response comparisons for the Flight 2 Mach 2 parameter identification maneuver.



050572

Figure 20. Aileron loop frequency response comparisons for the Flight 3 Mach 3 parameter identification maneuver.

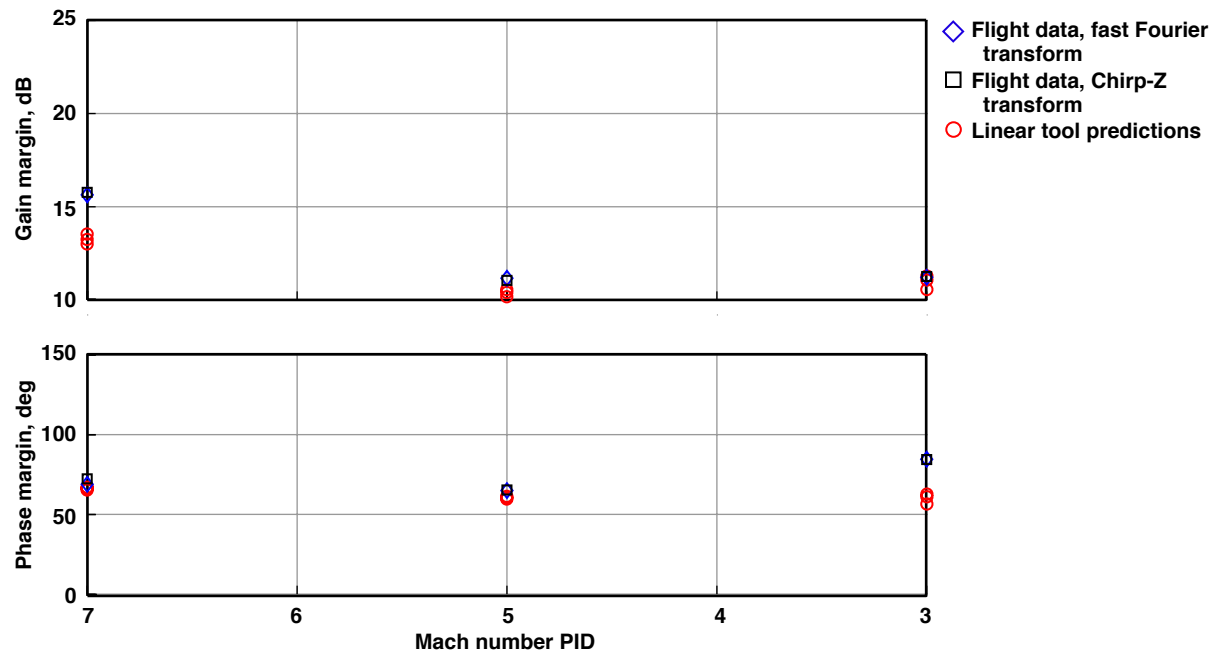
The aileron loop stability margin values for the HXRV during Flight 2 can be seen in figure 21. The gain and phase margin measurements for the Mach 5 through the Mach 3 PID are consistently higher than the linear predictions with differences generally up to 1.4 dB and 10 deg. The magnitude of these differences indicates a good correlation between the linear predictions and the in-flight measurements. The gain and phase margin measurements are as much as 4.25 dB and 12 deg higher during the Mach 2 PID than the predictions. This greater difference seen during the Mach 2 PID maneuver is caused by the shift in the gain response already discussed.



050573

Figure 21. Aileron loop stability margin estimates for Flight 2.

Figure 22 shows the stability margin comparisons for Flight 3. The Mach 7 PID showed gain margin differences of approximately 2.5 dB and phase margin differences of approximately 7 deg. The comparisons improved for the Mach 5 PID, while the Mach 3 PID shows a significant difference in the phase margin predictions. The coherence during this last aileron PID maneuver shows a slight decrease in the gain crossover region and the linear analysis tools predict a slightly different phase response in this area. The lower coherence estimate and slightly different phase response explains the increased differences when compared with linear analysis values.



050574

Figure 22. Aileron loop stability margin estimates for Flight 3.

CONCLUSION

Tailored input excitation signals were used in the X-43A flight test program to obtain control loop frequency responses during the post-engine test descent. The short time period of the excitation signals allowed for frequency responses and stability margins to be extracted at multiple flight conditions during the descent of the X-43A to the ocean. A problem with obtaining data for the rudder loops did not allow for valid frequency response data for each control loop at the same flight condition and thus precluded a multiple-input/multiple-output system analysis. The original premise of simultaneously applying excitation signals to multiple control loops still appears to be valid, because data were successfully obtained from the elevator and aileron control loops. The cause of the rudder and aileron loop interference is currently under investigation. The valid in-flight frequency response and stability margin values obtained for Flights 2 and 3 matched linear analysis predictions well, indicating a good understanding of the Hyper-X Research Vehicle aerodynamics and subsystems.

REFERENCES

1. Bosworth, John T., and Johnny C. West, "Real-Time Open-Loop Frequency Response Analysis of Flight Test Data," AIAA-1986-9738, 1986.
2. Schroeder, M. R., "Synthesis of Low-Peak-Factor Signals and Binary Sequences With Low Autocorrelation," *IEEE Transactions On Information Theory*, January 1970.
3. Young, Peter, and Ronald J. Patton, "Comparison of Test Signals for Aircraft Frequency Domain Identification," *Journal of Guidance, Control, and Dynamics*, Vol. 13, No. 3, 1990, pp. 430–438.
4. Bosworth, John T., and John J. Burken, *Tailored Excitation for Multivariable Stability-Margin Measurement Applied to the X-31A Nonlinear Simulation*, NASA Technical Memorandum 113085, 1997.
5. Morelli, Eugene A., "Multiple Input Design for Real-Time Parameter Estimation in the Frequency Domain," *13th IFAC Conference on System Identification*, Paper REG-360, 2003.
6. Reubush, David E., Luat T. Nguyen, and Vincent L. Rausch, "Review of X-43A Return to Flight Activities and Current Status," AIAA-2003-7085, 2003.
7. X-43A Mishap Investigation Board, *Report of Findings: X-43A Mishap*, Vol. 1, 2003.
8. Marshall, Laurie A., Griffin P. Corpening, and Robert Sherrill, "A Chief Engineer's View of the NASA X-43A Scramjet Flight Test," AIAA-2005-3332, 2005.
9. Marshall, Laurie A., Catherine Bahm, Griffin P. Corpening, and Robert Sherrill, "Overview With Results and Lessons Learned of the X-43A Mach 10 Flight," AIAA-2005-3336, 2005.
10. Morelli, Eugene A., Stephen D. Derry, and Mark S. Smith, "Aerodynamic Parameter Estimation for the X-43A (Hyper-X) from Flight Data," AIAA-2005-5921, 2005.
11. Davidson, J., F. Lallman, J. D. McMinn, J. Martin, J. Pahle, M. Stephenson, J. Selmon, and D. Bose, "Flight Control Laws for NASA's Hyper-X Research Vehicle," AIAA-1999-4124, 1999.
12. Norlin, Ken A., *Flight Simulation Software at NASA Dryden Flight Research Center*, NASA Technical Memorandum 104315, 1995.

REPORT DOCUMENTATION PAGE					<i>Form Approved</i> OMB No. 0704-0188	
<p>The public reporting burden for this collection of information is estimated to average 1 hour per response, including the time for reviewing instructions, searching existing data sources, gathering and maintaining the data needed, and completing and reviewing the collection of information. Send comments regarding this burden estimate or any other aspect of this collection of information, including suggestions for reducing this burden, to Department of Defense, Washington Headquarters Services, Directorate for Information Operations and Reports (0704-0188), 1215 Jefferson Davis Highway, Suite 1204, Arlington, VA 22202-4302. Respondents should be aware that notwithstanding any other provision of law, no person shall be subject to any penalty for failing to comply with a collection of information if it does not display a currently valid OMB control number.</p> <p>PLEASE DO NOT RETURN YOUR FORM TO THE ABOVE ADDRESS.</p>						
1. REPORT DATE (DD-MM-YYYY) 08-01-2007		2. REPORT TYPE Technical Memorandum			3. DATES COVERED (From - To)	
4. TITLE AND SUBTITLE Tailored Excitation for Frequency Response Measurement Applied to the X-43A Flight Vehicle				5a. CONTRACT NUMBER		
				5b. GRANT NUMBER		
				5c. PROGRAM ELEMENT NUMBER		
6. AUTHOR(S) Baumann, Ethan				5d. PROJECT NUMBER		
				5e. TASK NUMBER		
				5f. WORK UNIT NUMBER		
7. PERFORMING ORGANIZATION NAME(S) AND ADDRESS(ES) NASA Dryden Flight Research Center P.O. Box 273 Edwards, California 93523-0273					8. PERFORMING ORGANIZATION REPORT NUMBER H-2679	
9. SPONSORING/MONITORING AGENCY NAME(S) AND ADDRESS(ES) National Aeronautics and Space Administration Washington, DC 20546-0001					10. SPONSORING/MONITOR'S ACRONYM(S) NASA	
					11. SPONSORING/MONITORING REPORT NUMBER NASA/TM-2007-214609	
12. DISTRIBUTION/AVAILABILITY STATEMENT Unclassified -- Unlimited Subject Category 08 Availability: NASA CASI (301) 621-0390 Distribution: Standard						
13. SUPPLEMENTARY NOTES Baumann, Dryden Flight Research Center. Presented at the 44th Aerospace Sciences Meeting and Exhibit, January 9–12, 2006, Reno, Nevada.						
14. ABSTRACT An important aspect of any flight research project is assessing aircraft stability and flight control performance. In some programs this assessment is accomplished through the estimation of the in-flight vehicle frequency response. This estimation has traditionally been a lengthy task requiring separate swept sine inputs for each control axis at a constant flight condition. Hypersonic vehicles spend little time at any specific flight condition while they are decelerating. Accordingly, it is difficult to use traditional methods to calculate the vehicle frequency response and stability margins for this class of vehicle. A technique has been previously developed to significantly reduce the duration of the excitation input by tailoring the input to excite only the frequency range of interest. Reductions in test time were achieved by simultaneously applying tailored excitation signals to multiple control loops, allowing a quick estimate of the frequency response of a particular aircraft. This report discusses the flight results obtained from applying a tailored excitation input to the X-43A longitudinal and lateral-directional control loops during the second and third flights. The frequency responses and stability margins obtained from flight data are compared with preflight predictions.						
15. SUBJECT TERMS Frequency sweep, Hyper-X, Stability margin estimate, Tailored excitation, X-43A						
16. SECURITY CLASSIFICATION OF:			17. LIMITATION OF ABSTRACT	18. NUMBER OF PAGES	19a. NAME OF RESPONSIBLE PERSON	
a. REPORT	b. ABSTRACT	c. THIS PAGE			STI Help Desk (email: help@sti.nasa.gov)	
U	U	U	UU	29	19b. TELEPHONE NUMBER (Include area code) (301) 621-0390	